We are IntechOpen,
the world's leading publisher of
Open Access books
Built by scientists, for scientists

6,900
Open access books available

185,000
International authors and editors

200M
Downloads

154
Countries delivered to

Our authors are among the

TOP 1%
most cited scientists

12.2%
Contributors from top 500 universities

CLARIVATE ANALYTICS
BOOK CITATION INDEX
INDEXED

WEB OF SCIENCE™

Selection of our books indexed in the Book Citation Index
in Web of Science™ Core Collection (BKCI)

Interested in publishing with us?
Contact book.department@intechopen.com

Numbers displayed above are based on latest data collected.
For more information visit www.intechopen.com

Solar Cells with InGaN/GaN and InP/InGaAsP and InGaP/GaAs Multiple Quantum Wells

Shaoguang Dong, Kanghua Chen, Guojie Chen and Xin Chen

Additional information is available at the end of the chapter

1. Introduction

InGaN alloys materials are extensively utilized in light emitting diodes (LEDs) and laser diodes (LDs). In recent years, InGaN alloys materials have also been considered to use in solar cells because of their favorable photovoltaic properties, including a direct band gap, a higher absorption coefficient at the band edge, superior radiation resistance, high carrier mobility, thermal stability and so on. Especially, the band gap of the InGaN alloys materials can even vary from 0.7 eV to 3.4 eV, which covers almost the sun spectrum. [1] Additionally, four-junction tandem solar cells with a theoretical conversion efficiency of over 60% have been designed, but these designs require some junctions that have band gap of greater than 2.4 eV. Very few materials have a band gap of over 2.4 eV but InGaN alloys. Therefore, InGaN alloys are the candidate of using in highly efficient tandem solar cells.

Many challenges must be overcome before InGaN alloys can be used widely photovoltaic devices. A large lattice mismatch between GaN and InN atoms limits InGaN alloys using in photovoltaic devices in which these alloys must incorporate a thick absorb layer with high indium composition for absorbing incident light. Generally, the critical thickness of $In_{0.1}Ga_{0.9}N$ is approximately 100 nm, and this thickness falls rapidly as the indium composition increasing. When the thickness of InGaN alloys layer exceeds a critical value, defects are formed as recombination centers. These recombination centers increase the rate of consumption of photogenerated electron-hole pairs, degrading photovoltaic performance. Owing to the need for high crystalline quality, the thickness of absorb layers in InGaN alloys photovoltaic devices is limited by challenges related to epitaxial deposition such that a compromise of multiple quantum well (MQW) structure is used for the absorb layers in InGaN alloys photovoltaic devices, which results in insufficient light absorption.

Previous studies have utilized several methods for improving the collecting of light in InGaN/GaN MQWs solar cells, such as the use of a ZnO or SiO_2 sub-wavelength structure to realize a graded refractive index interface to reduce Fresnel reflection and simultaneously to increase the light scattering effect. Silver nanoparticles have also been used to exploit the surface plasmon effect to promote the scattering of light. However, because the light absorption is not sufficient, the lower external quantum efficiency and the higher absorption coefficient in the ultraviolet region have not been solved yet. [2]A back reflector that reflects the unused light back to the absorr layer provides a solution and has an important role in thin film solar cells. For this purpose, distributed Bragg reflectors (DBRs) are good candidates for InGaN/GaN MQWs solar cells.

Due to InGaN alloys materials have tunable band gaps and superior photovoltaic characteristics, they would be emerged as promising solar cells materials. [3] The band gap of InGaN alloys materials changed from 0.7 eV to 3.4 eV and these band gaps can be tuned by changing the contents of indium in the InGaN alloys materials. InGaN alloys mateials also have direct band gaps in the entire alloys range. For achieving higher photoelectric conversion efficiency, the multiple quantum wells solar cell structure has been proposed, which exhibits stronger absorption properties than bulk materials. [3] The quantum wells layers of the solar cells extend the absorption spectrum into the infrared region, in the case of radiant energy levels in the semiconductor band gap. The quantum wells similar to the p–i–n diode structure may extend the solar cells absorption spectrum, and then results in a higher short circuit current density (J_{sc}). The recombination rate of these quantum wells has been improved, which result in a higher open circuit voltage (V_{oc}). The finally result is that the photoelectric conversion efficiency (η) of the solar cells has been increased.

Group III–Nitride alloys materials solar cells are the better candidates for multiple quantum wells solar cells, because these alloys have direct band gaps and also have the better absorption of the solar spectrum. Recently, multi-junctions solar cells have been used to obtain higher conversion efficiency than single-junction solar cells. [3]However, the properties of lattice-matched quantum wells solar cells with different In content significantly complicate the fabrication process and design of the solar cells device. The average strain is chief when designing strained quantum wells solar cells. In order to maximize the absorption of quantum wells, it is better to maximize the carries concentration of quantum wells, the width and the number of quantum wells. In fact, all these factors increase the average strain, so the solar cells eventually become limited by the critical thickness. So the relative contributions of tunneling and thermionic emission currents of the multiple quantum wells structure are functions of the operation temperature and should provide guidance for the optimized design of multiple quantum wells solar cells tailored for operation in specific temperature ranges.

For the fabrication of InGaN alloys solar cells, there is considerable interest in the growth of GaN and InGaN alloys on Si substrates, because Si substrates have the advantages of low cost and large size. [4] Si substrates have a better thermal conductivity, whereas sapphire and SiC substrates have worse thermal conductivity. However, integration has been hampered by the large density of defects and cracks arising from larger lattice mismatch between GaN and Si.

Some studies have grown GaN on Si (100) or Si (111) substrates by adding buffers to overcome the larger density of defects and cracks. [5]

Recently most reported InGaN alloys solar cells have very low photovoltaic efficiency compared to Si-based solar cells. However, InGaN alloys materials superior resistance against irradiation damage makes themselves very suitable for the applications in photovoltaic devices, and motivates further development. In some investigations, GaN has usually been grown on sapphire or SiC substrates, which are expensive and difficult to integrate into the silicon industry. [3] Therefore, it is desirable to grow GaN on silicon substrate and integrate GaN with the mature silicon fabrication techniques.

The optoelectronic performance of InGaN solar cells devices are researched by preparing InGaN/GaN multiple quantum wells with In composition exceeding 0.3, attempting to alleviate to the phase separation phenomenon of InN and GaN materials at a certain degree by this InGaN/GaN multiple quantum wells structure. The InGaN/GaN multiple quantum wells solar cells have a better optoelectronic performance at wavelengths longer than 430 nm. The InGaN solar cells devices show better open circuit voltage (2.0 V) and external quantum efficiency (45%) and high fill factor (65%) because of the InGaN/GaN multiple quantum wells structure.

Recently, concentrator systems solar cells are becoming a main technology for the large scale electrical power by utilizing high conversion efficiency group III–V multi-junctions solar cells. Sharp's triple-junctions InGaP/GaAs/InGaAs concentrator solar cells have got a high conversion efficiency of 44.4% under about 300 suns. [6] The solar cells will probably to be four or more junction cells with higher conversion efficiency in the future. The ideal highest conversion efficiency is 55% for four-junctions solar cells, which could be achieved by utilizing an optimized band gap combination of 1.9/1.4/1.0/0.7 eV. [6]The four-junctions solar cells is a promising photovoltaic candidate devices because of the bandgap combination of InGaP/GaAs (1.9/1.4 eV) which matched to GaAs in their lattice and that of InGaAsP/ InGaAs (1.0/0.7 eV) which matched to InP in their lattice.

Currently, only a few contributions have been reported on InGaAsP materials solar cells grown by metal organic chemical vapor deposition (MOCVD). In fact, InGaAsP materials solar cells can also be grown by molecular beam epitaxy (MBE), which can give more precise growth control technology. Researcher ever think that the photovoltaic performance of solar cells grown by MBE method is not probably better than MOCVD growth methods, because the growth temperature of MBE methods is very lower, which results in more defect states and deep defect centers in bulk materials. Recently, a high efficiency GaInP/GaAs/GaInAsN triple-junctions solar cell was successfully grown by MBE methods. [6]The experimental results showed that the solar cells containing group III–V materials grown by MBE growth are as good as the MOCVD growth. It has been a challenge to grown a high quality InGaAsP materials which bandgap is only 1.0 eV on an InP substrate by MBE methods. Furthermore, a comprehensive study on the carrier recombination dynamics of InGaAsP material grown by MBE has not been reported.

The solar cells of InP/InGaAsP double hetero-junction (DH) structure have been investigated and compared these solar cells to the InP control cells. [7] The InGaAsP has many band gap values from 0.75 eV to 1.35 eV which very matched to the InP in lattice. The InP/InGaAsP double hetero-junction structure solar cells whose light absorption layer is the InGaAsP has also been investigated. [7] The investigated results are that the InP/InGaAsP double hetero-junction structure solar cells have a lower open-circuit voltage and the short-circuit current improves twice compared to the InP control cells. So the InP/InGaAsP double hetero-junction structure can greatly improve the conversion efficiency of the solar cells.

The photoelectric performance of InP/InGaAsP multiple quantum wells solar cells are improved by light scatter coming from deposited dielectric or metal nanoparticles. [8]The integration of dielectric or metal nanoparticles on the multiple quantum wells solar cells showed that incident light can enter the bulk by lateral optical propagation paths, and the refractive index can provide the optical confinement between the quantum well layers and surrounding materials layers. By the materials surface optimization of silica and Au nanoparticle, short-circuit current density could be increased by 12.9% and photoelectric conversion efficiency also could be increased by 17%, respectively.

Group III–V compound multi-junctions solar cells have the advantage for achieving photoelectric conversion efficiency exceed to 40%, and they are also a promising photovoltaic materials for the space and terrestrial solar cells devices. [9] Among the multi-junctions solar cells technologies, the double-junctions solar cells is the simplest structure and has attracted extensive interesting for further optimizing these solar cells device performance. One of the most trusted materials is the GaInP/GaAs alloys system whose band gap is 1.9 and 1.4 eV respectively. When GaInP materials are acted as the top cell, many problems of bulk defects and crystal quality found existing in other alloy materials such as AlGaAs can even be avoided.

As a result, the researches on the GaInP and GaAs materials property have been become very important, especially the study on the recombination dynamics of carriers in the active layers. For example, surface recombination velocity of the GaInP layer could be measured by the intensity of photoluminescence, and the effective lifetime of minority carriers of the GaInP or GaAs layer could be also measured by the intensity of photoluminescence. On the other hand, the characterization of carrier dynamics and the loss of carriers have been reported little from references. Despite the electroluminescence measurement has been used for modeling the irradiation-induced degradation of the multi-junctions solar cells structures in space conditions, compared with the photoluminescence technique, it is believed that the electroluminescence measurement is also competent in revealing detailed the kinetics of the recombination loss of carriers. InGaP solar cells which have about 1.9 eV band gap and lattice-matched to GaAs, have been used for the top cells of multi-junctions solar cells.

InGaP/GaAs/InGaAs multi-junctions solar cells have been achieved high conversion efficiency of 36.4% under AM1.5. Recently, the intermediate band solar cells have been extensively studied and providing a high conversion efficiency of over 60% under concentrated sunlight conditions. [10]The intermediate band is formed by the quantum dot superlattice in intermediate band solar cells, which located in the bandgap and used to absorb the sub-bandgap photons in the intermediate band state. To achieve a conversion efficiency of more than 60%,

the materials with a bandgap of about 1.9 eV are needed. However, the quantum dot super-lattice solar cells have used GaAs semiconductor materials whose bandgap is only 1.4 eV. In order to realize intermediate band solar cells with a conversion efficiency of over 60%, a wide bandgap semiconductor material is needed. In fact, InGaP is a suitable intermediate band material with bandgap of 1.9 eV. [10]

InGaP material is very difficult to grow by the solid-source molecular beam epitaxy technique which is suitable for growing a high quality quantum dot structure. The InGaP epitaxial layers are required to obtain sufficient light absorption in the solar cells devices, a large-scale phosphorus source are needed in the molecular beam epitaxy chamber. In fact, all of most InGaP solar cells are grown by metal organic chemical vapor deposition.

An InGaP/GaAs tandem solar cell of 4 cm^2 larger area is realized, which got a new conversion efficiency record of over 30% under AM 1.5. [11]Those tandem solar cells performances were improved by utilizing InGaP tunnel junction and a double hetero-junctions structure, where the InGaP layers are surrounded by AlInP barrier layers. The double hetero-junctions structure increased the peak current value of InGaP tunnel junction. The AlInP barrier layer takes the part of a back surface field; it is found that the AlInP barrier layer can effectively reflect minority carriers in the InGaP top cells. The AlInP barrier layer has a high potential and can prevent the diffusion of zinc from a doped tunnel junction toward the top cells during growth. Further-more, the InGaP tunnel junction can also reduce the light absorption loss and increase the photogenerated current in the GaAs bottom cell. [11]

The photoelectric conversion efficiency of InGaP/GaAs/Ge multi-junctions solar cells has been technically improved up to 32% under AM1.5. The InGaP material is on first hetero-junction growth layer, combined with Ge bottom layer and double hetero-junction tunnel junctions, in which Ge substrate is precisely matched with the conventional GaAs in their lattice structure. If the AlInGaP material whose band gap is 1.95 eV is employed in the top cells layer, the conversion efficiency of these solar cells should be improved further. Furthermore, thin film structure of InGaP/GaAs solar cells on metal film has been reported. The thin film solar cells of InGaP/GaAs are founded lightweight, high flexibility, high radiation resistance and high efficiency.

The use of multiple quantum wells is very advantageous in the conventional tandem solar cells, because multiple quantum wells can independently tailor the absorption edge of each cell, which has no such problem of lattice mismatch and relaxation. [12]The InGaP/GaAs solar cells was improved by using strain balanced multiple quantum wells; the multiple quantum wells structure of tandem solar cells has achieved the conversion efficiency of over 30% under AM1.5. This conversion efficiency is a new record for currently photovoltaic devices. The conversion efficiency of over 34% could be realized under AM1.5 by optimizing the solar cells device structure. The possibility and gains are currently researched by introducing multiple quantum wells structure into top cells and bottom cells layer of an InGaP/GaAs solar cells device.

2. InGaN/GaN MQWs solar cells

InGaN alloys semiconductor materials as active layers of light emitting diodes have been widely investigated, which emission wavelengths cover from red to near ultraviolet spectral regions. [13] Recently, InGaN alloys as a new solar cells materials have been interested by their tunable energy band gaps which vary from 0.7 eV to 3.4 eV, covering almost the whole sunlight spectrum, and also their superior photovoltaic characteristics, such as high carrier mobility, direct energy band gap, high optical absorption coefficient near the band edge, high drift velocity and low radiation resistance. [14]

Although InGaN alloys material solar cells offer tremendous potential for photovoltaic applications, there are only a few references on InGaN alloys solar cells. Furthermore, most of reported InGaN alloys solar cells usually have In contents no more than 15% and band gaps about 3.0 eV or larger, therefore, external quantum efficiency is nearly not exist at wavelengths longer than 420 nm. [15] An earlier theoretical calculation has been indicated that the use of a special active material in solar cells can obtain conversion efficiency greater than 50%, that material is InGaN alloys whose In content exceed 40%. [16]Additionally, group III-nitride multi-junction solar cells with ideal band gaps for maximum conversion efficiency must be incorporated InGaN alloys with higher In contents. [13]

In this section, the optoelectronic properties of InGaN alloys solar cells are researched by merging into InGaN/GaN multiple quantum wells (MQWs), attempt to alleviate the phase separation issue of InN and GaN in a certain extent, and demonstrate the photovoltaic performance of solar cells operating in wavelengths longer than 420 nm.

2.1. MQWs solar cells layers structure

The MQWs solar cells layers structure fabricated by InGaN alloys and GaN materials is shown in Figure 1, the light absorption region consists of eight periods of InGaN (3 nm)/GaN (8 nm) MQWs. The MQWs were grown under the established MOCVD growth conditions; InGaN alloys materials with In content about 0.3 or 0.4 work in longer wavelengths in order to obtain better photovoltaic responses. The thickness of p-GaN or n-GaN is about 150 nm. The device structure was grown on a GaN/Al_2O_3 template. As demonstration, the device fabrication steps are adopted to commercial group III-nitride LEDs and implemented a thin Ni/Au semitransparent current spreading layer to minimize the p-contact resistance on the p-GaN window layer.

The growth of high quality crystalline structure InGaN alloys materials is highly challenging in all of In composition range. One of the main problems is that the lattice is seriously mismatched between InN and GaN atoms, resulting in low solubility and phase separation between InN and GaN materials. [17]Recently, single crystalline phase InGaN alloys materials with all of In composition range could be grown by metal organic chemical vapor deposition (MOCVD) by directly depositing on GaN templates without using buffer layers. [18] These InGaN alloys characteristics are illustrated in Figure 2, in which X-ray diffraction data of the (002) plane for several InGaN alloys materials for θ-2θ scans are shown. All scanned curves
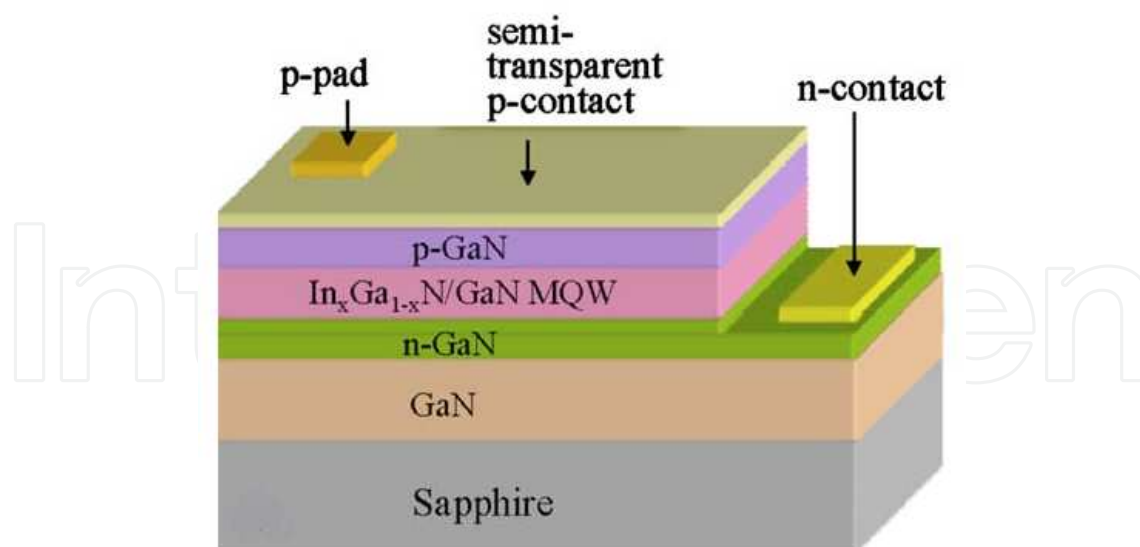
Figure 1. Schematic of layers structure based on InGaN/GaN MQWs solar cells.

exhibit no multiple peaks except for closing the InN peak position, showing that InGaN alloys materials have not been phase separation. The results show a significant growth improvement of InGaN alloys materials by MOCVD. [13]
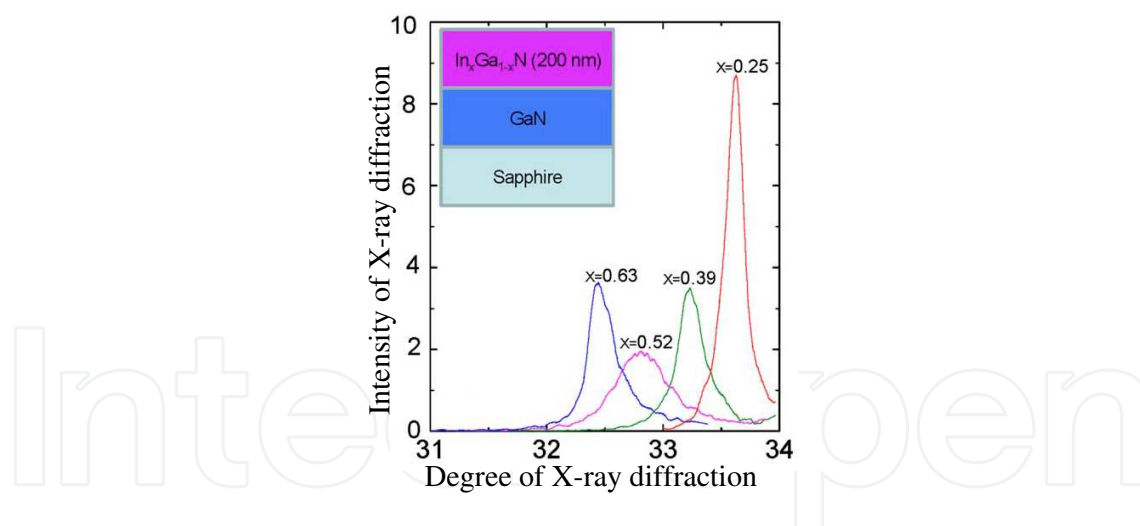

Figure 2. X-ray diffraction data for θ-2θ scan curves of the (002) plane

However, when In composition range exceed to the 0.5, the homogeneity of InGaN alloys materials is pretty poorer. The full width at half maximum of the θ-2θ-scans rocking curves of the (002) plane increases from about 1000 arcsec when In composition is 0.2 to about 3000 arcsec when In content is 0.5 for InGaN alloys materials of 200 nm thickness. The photoluminescence (PL) emission spectrum of InGaN alloys materials also is deteriorated with an increase of In composition, as shown in Figure 3. The intensity of PL emission spectrum of $In_{0.4}Ga_{0.6}N$ alloys is about 100 times lower than that of $In_{0.2}Ga_{0.8}N$. This trend of crystalline

quality reduced with In composition increasing makes the realization of solar cells based on InGaN alloys materials with In content greater than 0.3 highly challenging. Evidence that strain could suppress phase separation in InGaN alloys materials has been reported. [19] It was shown that InGaN alloys materials with In content lower than 0.5 without phase separation can be grown when the alloys is embedded by an InGaN/GaN double heterostructure.
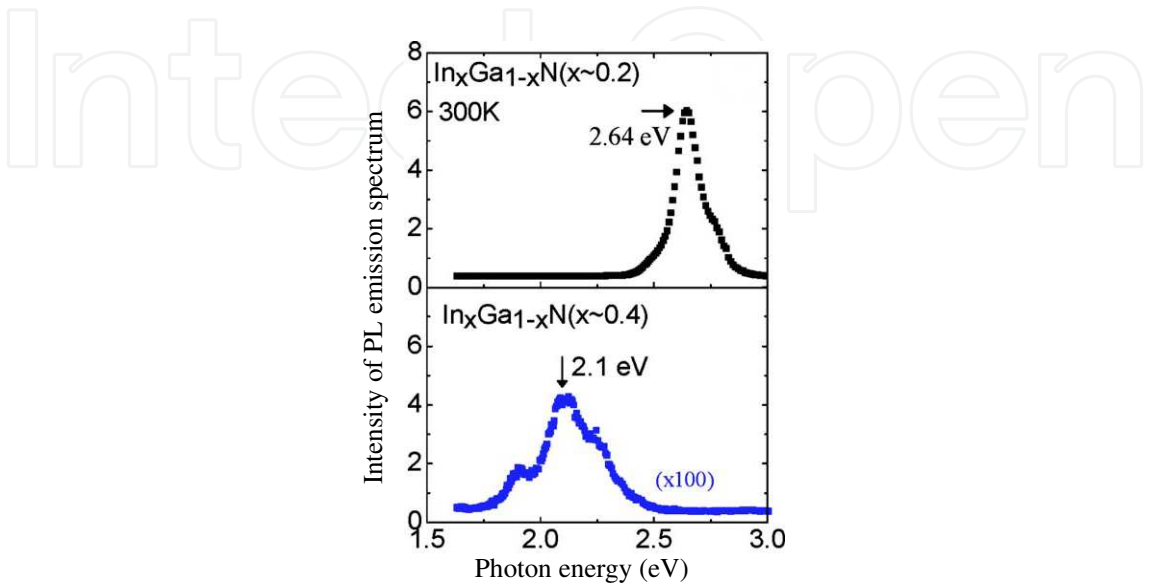

Figure 3. PL emission spectrum of InGaN alloys materials grown on GaN/Al$_2$O$_3$ templates.
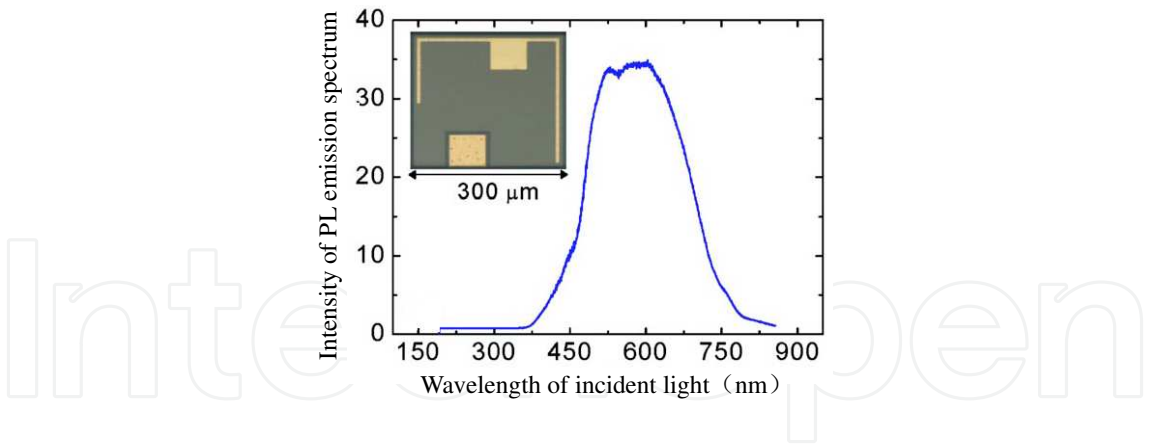
Figure 4. Emission spectrum of the white light source and the inset is the microscopy image of MQWs solar cells.

2.2. MQWs solar cells performance

An optical microscopy image of a MQWs solar cells fabricated by InGaN alloys materials is shown in the inset of Figure 4. The MQWs solar cells were characterized by a microprobe station with a Keithley 2400 source meter. The solar cells were illuminated by a white light source with no optical filters to measure the current versus voltage characteristics, whose PL emission spectrum is shown in Figure 4. The solar cells were illuminated monochromatically

by using the same white light source to achieve the characterization of quantum efficiency versus excitation wavelength.[13]The PL emission spectrum for MQWs solar cells structure fabricated by InGaN alloys materials with In content about 0.3 and GaN is shown in Figure 5, and exhibits an PL emission peak about 472 nm.
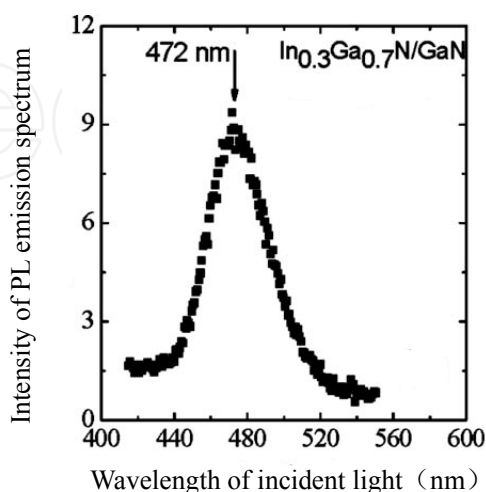

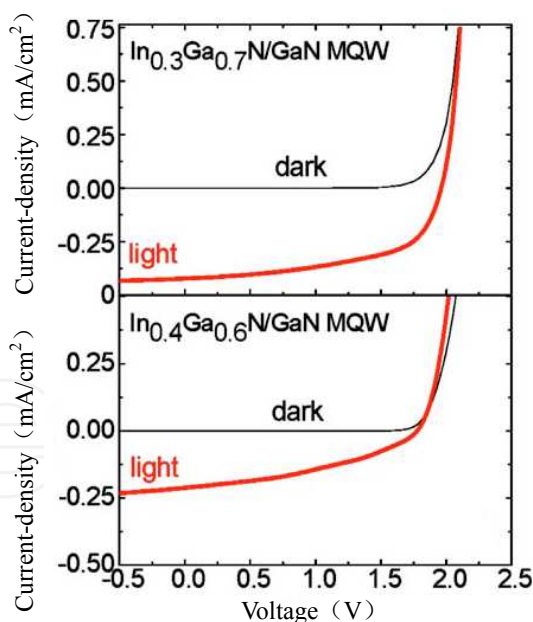**Figure 5.** PL emission spectrum of an InGaN/GaN MQWs solar cells structure.

Figure 6. Curves of *I-V* characteristics for In$_x$Ga$_{1-x}$N/GaN MQWs solar cells.

Current versus voltage (*I-V*) characteristics of two MQWs solar cells fabricated by InGaN alloys materials with In composition about 0.3 or 0.4 in the quantum well region and GaN are shown in Figure 6. The open-circuit voltage (*V*$_{oc}$) is about 2.0 V or 1.8 V for two MQWs solar cells with In composition about 0.3 or 0.4, respectively. These values are in good agreement with the

band gaps of $In_{0.3}Ga_{0.7}N$ and $In_{0.4}Ga_{0.6}N$. However, the performance of the solar cells with $In_{0.4}Ga_{0.6}N$/GaN MQWs as active region is no more than that of the solar cells with $In_{0.3}Ga_{0.7}N$/GaN MQWs, despite the $In_{0.4}Ga_{0.6}N$/GaN MQWs solar cells active layers are shown to have a much better spectral overlap with the excitation light source. [3]This degradation of these solar cells performance and the X-ray diffraction results are shown in Figure 2 and it is a direct reason of the InGaN alloys materials quality degradation with In composition increasing, which further leads to much loss of the photogenerated carriers. The observed photovoltaic characteristics of these solar cells are consistent with the quantum efficiencies of group III-nitride green LEDs which are much lower than those of blue LEDs. [13]
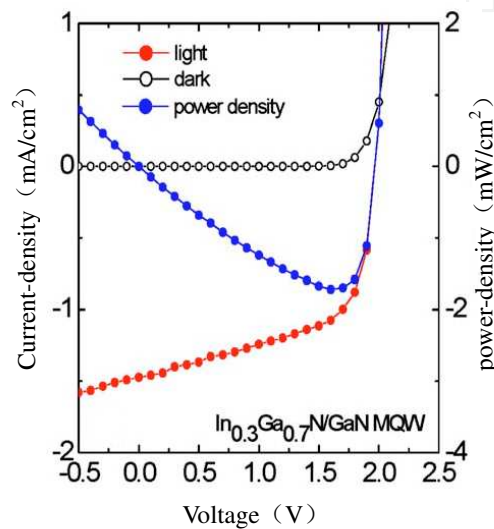

Figure 7. Curves of current-density vs voltage and power-density vs voltage.

Current density versus voltage and power density versus voltage curves of the solar cells with $In_{0.3}Ga_{0.7}N$/GaN MQWs as active layer are shown in Figure 7, a fill factor of over 60% is obtained from the solar cells. The external quantum efficiency as a function of excitation wavelength for the $In_{0.3}Ga_{0.7}N$/GaN MQWs solar cells is shown in Figure 8, from which we can see that the solar cells have an external quantum efficiency of 40% at 420 nm. The spectrum response is limited by using p-GaN window in the shorter wavelength region, and it would be improved if the p-AlGaN or p-InAlGaN material is incorporated. [13]Three major factors limited the external quantum efficiency are the following: (1) Light absorption in the semi-transparent p-contact layer. Current spreading in p-contact layer was only adopted from LED structure and the p-contact layer need to be optimized for solar cells devices. (2) The thickness of light absorption layer is too thin in the $In_{0.3}Ga_{0.7}N$/GaN MQWs structure. The well thickness and period of the $In_{0.3}Ga_{0.7}N$/GaN MQWs active region need to be optimized to maximize light absorption and minimize other detrimental effects, which is incorporated by relatively high In composition InGaN alloys materials in the multiple quantum well region. (3) InGaN alloys materials with relatively high In composition are very low crystalline quality. Nevertheless, the InGaN alloys materials solar cells have good external quantum efficiency working at such long wavelengths, so the MQWs is a effec-

tive method to design MQWs solar cells by InGaN alloys materials with relatively high In compostion for high photoelectric conversion efficiency. [13]
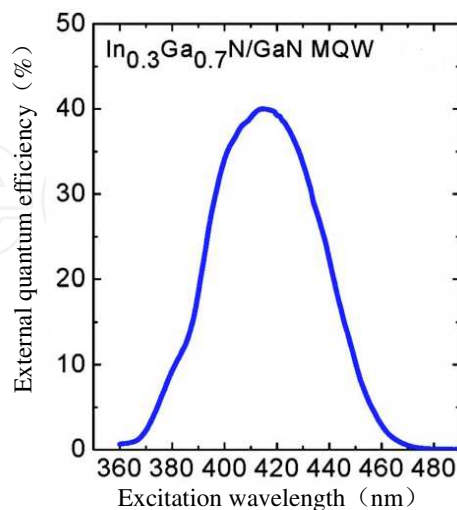

Figure 8. Curves of external quantum efficiency vs excitation wavelength.

3. InP/InGaAsP MQWs solar cells

Currently, there are extensively interests in the application of multiple quantum wells structure in solar cells devices; their optoelectronic conversion efficiency can exceed the single-junction solar cells theoretical efficiency limit of 31%. [20]Theoretically, maximum optoelectronic conversion efficiency range in multiple quantum wells solar cells could be predicted from 50% to 65%. The incorporation of multiple quantum wells structure can ensure high energy photon absorption efficiency and improved short-circuit current density (J_{sc}) and reduced in open-circuit voltage (V_{oc}), because no enough collection efficiency of photogenerated carriers is especially obvious. [21] Regardless of these problems, the maximum power of multiple quantum wells solar cells devices can exceed that of the similar homo-junction solar cells devices by extending the absorption spectrum to longer wavelengths. [22]We have got a conclusion that incident light can be normally got into lateral optical propagation paths in the multiple quantum wells solar cells devices by scattering from metal or dielectric nanoparticles, whose optical confinement is provided by the refractive index contrast between the quantum wells layer and surrounding materials. Substantially, the photogenerated current generation and collection over a large range of incident light wavelengths has been improved, particularly at longer wavelengths. [8]

3.1. MQWs solar cells *p-i-n* structure

The lattice matched InP/InGaAsP multiple quantum wells *p-i-n* structure solar cells is nominally shown in Figure 9. The *n*-type electrode of all *p-i-n* structures solar cells consist of a S

doped InP substrate with doping concentration about 5×10^{18} cm^{-3}, while the intrinsic region consist of 10 nm In$_{0.91}$Ga$_{0.09}$As$_{0.2}$P$_{0.8}$ barriers alternating with 10 nm In$_{0.81}$Ga$_{0.19}$As$_{0.4}$P$_{0.6}$ quantum wells for ten periods with an additional 50 nm or 25 nm In$_{0.91}$Ga$_{0.09}$As$_{0.2}$P$_{0.8}$ barrier on the top quantum wells layer. The *p*-type electrode of all *p-i-n* structures solar cells consist of a Zn doped 50 nm *p*-type InP layer or 25 nm *p*-type InP and 10 nm *p*-type In$_{0.47}$Ga$_{0.53}$As with doping concentration about 3×10^{18} cm^{-3}. The *n*-type Ohmic contacts were fabricated by using Ti (40 nm)/Au (200 nm) metal deposited by electron beam evaporation. 2 mm^2 window regions were formed by conventional photolithography, and *p*-type contacts were formed by using Ti (20 nm)/Pd (20 nm)/Au (200 nm) metal deposited by electron beam evaporation. [8]The top In$_{0.47}$Ga$_{0.53}$As contact layer was removed from the window region by a selective wet etch (H$_2$SO$_4$:H$_2$O$_2$:H$_2$O, 1:10:220) for 15 s, and about 15 nm SiO$_2$ surface passivation layer was sputter deposited over the window area of all devices.
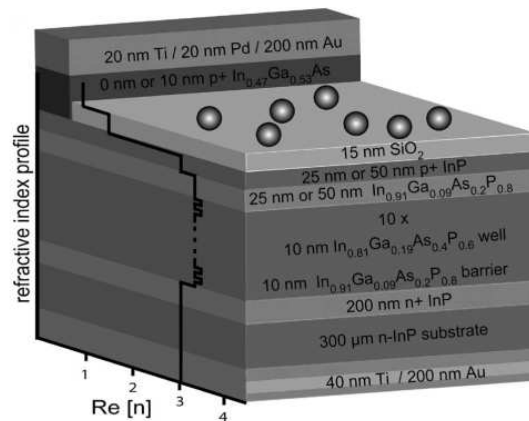

Figure 9. InP-based multiple quantum well solar cells with nanoparticles on the surface

To optimize collection efficiency of photogenerated carriers in the multiple quantum wells and to minimize the reduction of V_{oc}, a sufficiently large electric field across the intrinsic region is definitely required, in which the electric field intensity is 30 kV/cm or so, [23] and the barriers must be thermally or optically excited usually at 200~450 meV or less. [24] The electric field condition requires that the intrinsic region in the *p-i-n* structure should be especially thin, where the intrinsic region is required by choosing appropriate materials for the multiple quantum wells and barrier. [8]For the solar cells device structure with an intrinsic layer thickness of 250 nm, shown in Figure 9, the quantum wells electric field intensity is about 48 kV/cm at equilibrium condition, and 32 kV/cm at a maximum power state when operating voltage is about 0.4 V.

Incorporation of the multiple quantum wells region in solar cells device, not only improves photon absorption efficiency at longer wavelengths, but also increases the refractive index in the intrinsic region relative to the surrounding electrode contact layers, as also shown in Figure 9, which produces a slabby waveguide structure. [25] Waveguide mode accompanied by light scattered from metallic nanoparticles has been demonstrated by metal nanoparticles on silicon-on-insulator photodetectors. [26] The scattering effect is achieved by depositing metal

nanoparticles or dielectric nanoparticles at top of the solar cells device, as shown in Figure 10. The incident light scattered by the nanoparticles not only can improve transmission of photons into the solar cells active layers, but also make normally incident photons into lateral confined paths in the multiple quantum wells waveguide layer, result in photon absorption efficiency increasing, more photocurrent generating and optoelectronic conversion efficiency improving. [8]
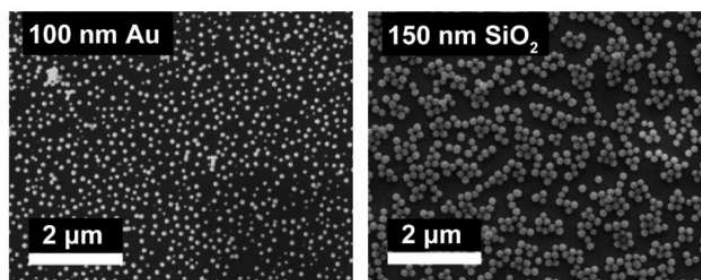

Figure 10. SEM images of 100 nm diameter Au nanoparticles (left) and 150 nm diameter SiO_2 nanoparticles (right).

3.2. MQWs solar cells *p-i-n* performance

The photocurrent response is shown in Figure 11 for an InP homojunction control device, a *p*-InP/ *i*-$In_{0.91}Ga_{0.09}As_{0.2}P_{0.8}$ /*n*-InP barrier control device, and a *p-i-n* multiple quantum wells solar cells device. These epitaxial layer structures for the control device and barrier control device and multiple quantum wells device were grown on 225 nm thicknesses intrinsic layer under identical reactor conditions. The photocurrent response only extends to 950 nm of the InP absorption edge for the InP homojunction control device, which is determined by room temperature photoluminescence measurements, but the photocurrent responses can extend to 1050 nm of the $In_{0.91}Ga_{0.09}As_{0.2}P_{0.8}$ absorption edges and 1150 nm of $In_{0.81}Ga_{0.19}As_{0.4}P_{0.6}$ absorption edges for the barrier control device and multiple quantum wells solar cells device, respectively.
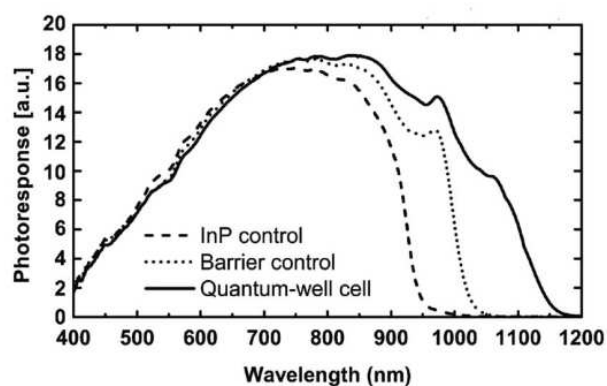

Figure 11. Photocurrent response spectra for InP homojunction device, barrier device and quantum well solar cell device

The maximum power curves are shown in Figure 12 for InP homo-junction control device, p-InP/i-In$_{0.91}$Ga$_{0.09}$As$_{0.2}$P$_{0.8}$/n-InP barrier control device and p-i-n multiple quantum wells solar cells device which all grown on 250 nm intrinsic layer thicknesses. Despite V_{oc} drops to 0.63V for the homo-junction control device and barrier control devices, and drops to 0.53 V for the quantum wells solar cells device, the maximum power output of the quantum wells solar cells device increases 7.4% and 4.6% relative to the homo-junction control device and barrier control device, respectively. [8]
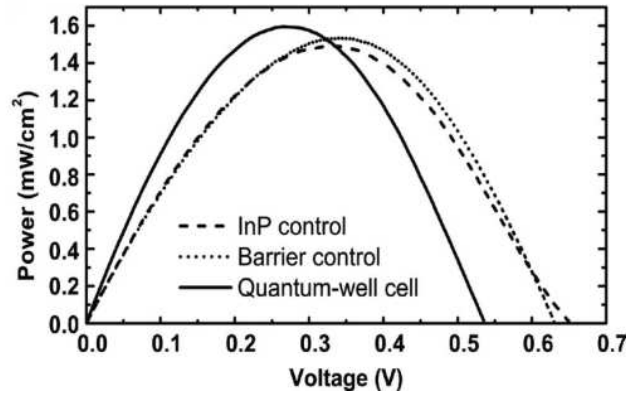

Figure 12. Power output curves for InP control device, barrier control device and quantum wells solar cells device
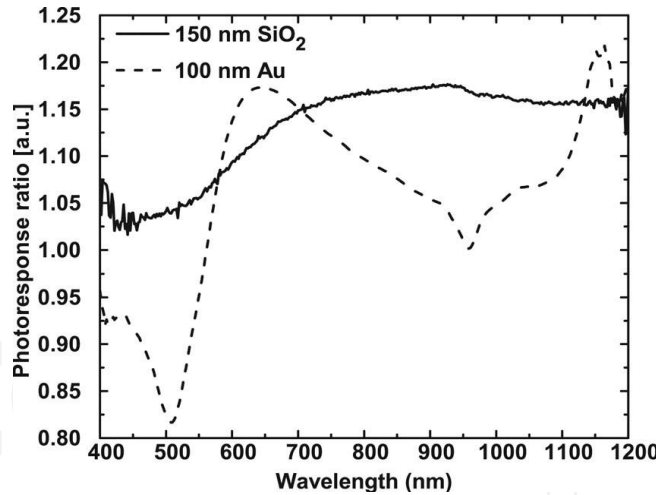

Figure 13. Photocurrent response spectra of quantum well solar cells with Au nanoparticles and SiO$_2$ nanoparticles

To illustrate the effect of nanoparticle scattering on the solar cells device in improved photo-current response and optoelectronic conversion efficiency, Figure 13 shows photocurrent response spectra for quantum wells solar cells with either 100 nm diameter Au or 150 nm diameter SiO$_2$ nanoparticles deposited on these solar cells surface, which plotted by photo-current response ratios relative to the spectrum for the solar cells device without nanoparticles. Au and SiO$_2$ nanoparticles densities were employed with about 2.7×10^9 cm^{-2} and 2.1×10^9 cm^{-2},

respectively. The nanoparticles deposition proceeding and photocurrent measurement apparatus are described in reference [27]. The incident light scattered by Au nanoparticles leads to a reduction of photocurrent response at wavelengths about 560 nm, at the same time, a phase shift is accompanied in the scattered wavelength near the nanoparticle plasmon resonance, which results in partially destructive interference between the scattered waves and the transmitted waves. [28] The scattering of incident light by the nanoparticles arise a broad wavelength range increased from 560 nm to 900 nm. But no surface plasmon polarization resonance is present for the SiO$_2$ nanoparticles, and the transmission and photocurrent response are increased over the range from 400 nm to 1200 nm wavelengths. [29]

The photocurrent response is increased at near 960 nm and cut off at about 1200 nm for the solar cells devices deposited by Au nanoparticles. This phenomenon is attributed to the scattering of incident light into optical propagation path modes, which associated with the slabby waveguide formed by the multiple quantum wells region and surrounding p-layers and n-layers. [8]A standard calculation shows that the slabby waveguide supports two confined modes at 960~1200 nm wavelengths range. [30]Furthermore, the optical waveguide structure mode becomes better confined with increasing wavelength because of the dependence of the wavelength and semiconductor refractive indices, resulting in the waveguide modes efficiency increased. [26]The photocurrent response is improved in these wavelength ranges because of incident light coming into the waveguide mode, and substrate radiation modes leads to photon propagation path lengths increased dramatically within the multiple quantum wells region that associated with lateral photon propagation path rather than vertical path. Consequently, the efficiency of photon absorption is improved greatly. [8]
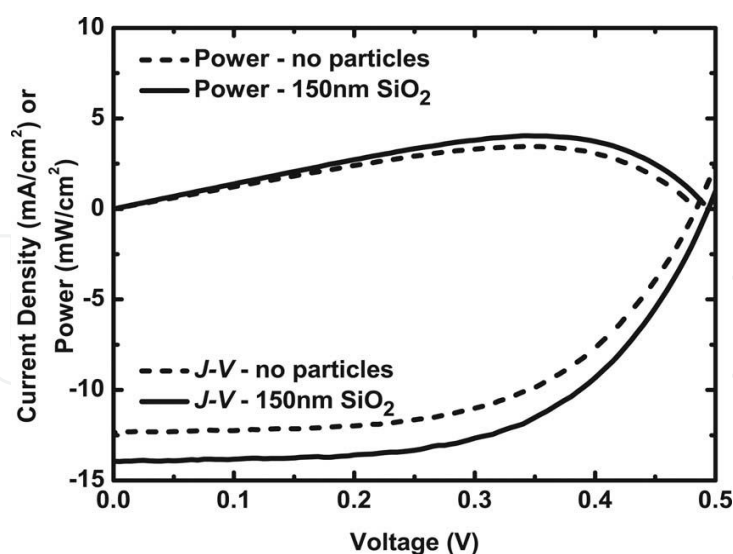

Figure 14. *J-V* and *P-V* curves measured for quantum well solar cell with and without SiO$_2$ nanoparticles

Previously, some groups have reported that the short circuit current density and optoelectronic conversion efficiency are increased due to optical scattering from metal nanoparticles deposited on Si solar cells [31] and *a*-Si solar cells [32]. The photocurrent response is enhanced on

the surface deposited nanoparticle quantum wells solar cells, which leads to the short circuit current density and optoelectronic conversion efficiency improved greatly under normal illumination incidence provided by a solar simulator with a Xenon arc lamp. The short circuit current density and voltage and the power output and voltage characteristics are shown in Figure 14 for the multiple quantum wells solar cells deposited SiO_2 nanoparticles on the surface before and after. For a SiO_2 nanoparticle surface density about 2.1×10^9 cm^{-2}, the short circuit current density increased 12.9% and maximum power conversion efficiency increased to 17.0%. For Au nanoparticle surface density about 2.7×10^9 cm^{-2}, the short circuit current density increased 7.3% and maximum power conversion efficiency increased only 1%.

The conversion efficiency and photocurrent response are improved substantially for the solar cells device structures whose quantum wells region bound with a lower refractive index substrate. A model developed by Soller and Hall [33] shows that when a horizontal electric dipole is located on a silicon insulator substrate, an excess of 80% of the light emitted by the electric dipole is coupled into the waveguide modes of the high refractive index Si insulator layer. [34]The ratio of the power of the electric dipole into waveguide modes fully to the total power of the electric dipole for the solar cells device structure over 600~1200 nm wavelengths occurs with a maximum efficiency no more than 10% in the course of the emission into waveguide, and leaky modes is in the range of 85~90%. This low efficiency is due to the small refractive index contrast to the solar cells device structure and could be improved with greater refractive index. [8]

4. InGaP/GaAs MQWs solar cells

Concentrators have the advantage to reduce the cost of photovoltaic systems by collecting the direct photon component with inexpensive lenses. The economic benefits of the concentrators demand a lot of high efficiency solar cells and the application of a nanostructure technology to these photovoltaic materials. GaAs materials provide the highest conversation efficiency in single-junction solar cells in all concentrations. However, the bandgap of GaAs is 1.42 eV and higher than the 1.1 eV of optimal efficiency bandgap at the conditions of high concentration. [35]Strain balanced InGaAs quantum wells in the intrinsic region of GaAs single junction solar cells can extend the absorption edge in substrate devices. [36] The result of increasing short circuit current accompanied with drop in open circuit voltage and increasing efficiency prevails over comparable conventional solar cells. [37]

An optimum of similar band gap can also exist in the case of two junction tandem solar cells. The efficiency record is 30.2% for the InGaP/InGaAs tandem solar cells at 300 times concentration. [12] However, as shown in Figure 15, the bandgaps combination of 1.8 eV/1.42 eV of an InGaP/GaAs tandem solar cells is significantly higher than the optimum bandgaps combination under 500 times concentration. Approaches have being actively pursued to lower the bandgaps of tandem solar cells, including lattice mismatched dilute nitrides InGaP/InGaAs grown on a virtual substrate. [38] These introducing dislocations can lower the voltage of the tandem solar cells, though the efficiency record has achieved about 42 % by the virtual

substrate approach. [39] Strain balanced quantum wells in InGaP/InGaAs tandem solar cells may allow the absorption edge of top and bottom cell to be adjusted independently without existing relaxation and lattice mismatch. [40] If there is enough absorption in the strain balanced quantum wells of top and bottom cell, the conversion efficiency of InGaP/InGaAs tandem solar cells device could ascend along the contours in Figure 15 and be adjusted to the solar spectrum. [12]Dark line shows the bandgaps of GaInP and GaAs. The red-cross shows the bandgaps position of the strain balance quantum wells tandem solar cells and the blue star shows a proposed structure with quantum wells in two junction solar cells.
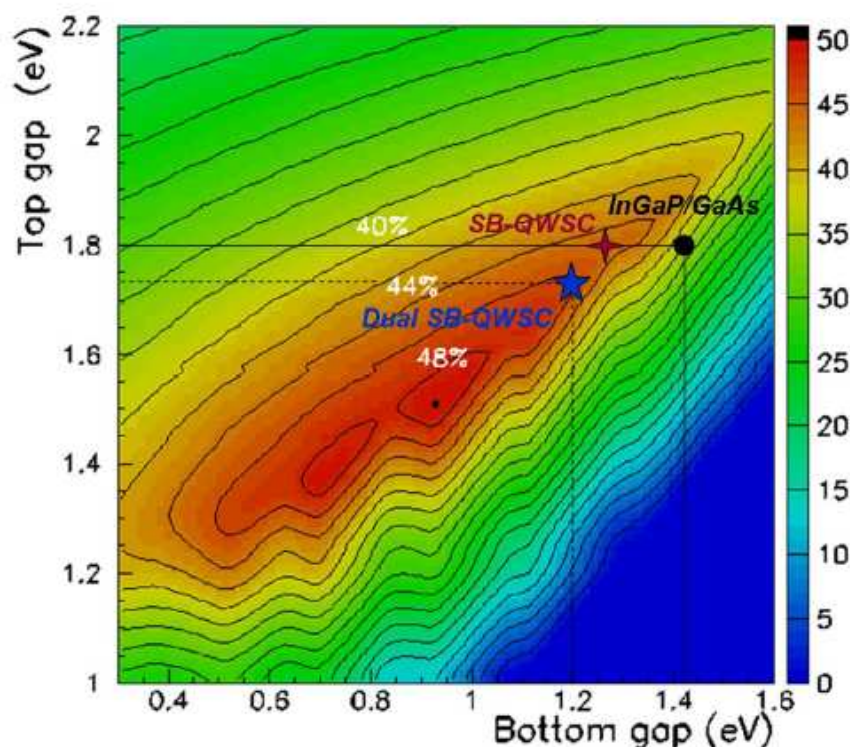

Figure 15. Ideal conversion efficiency contour plot for tandem solar cells under 500 times concentration

4.1. SBQW solar cells layers structure

Many quantum wells can be grown in the intrinsic layers of the *p-i-n* solar cell without dislocations and relaxation [41] by strain balancing the pressure imposed by the lower lattice spacing of InGaAs quantum wells and the higher lattice spacing of GaAsP barrier materials. [42]The strain balancing (SB) method and a resultant energy band diagram are shown in Figure 16.

All the solar cells devices were fabricated by metal organic vapour phase epitaxy (MOVPE). The InGaP/GaAs tandem solar cells were grown on the bottom cell where quantum wells in the intrinsic region of it. The second cell was top cell with higher emitter doping and lower In content in quantum wells. In the two cells, the bottom cell was grown by III-V growing technologies. The top cell was grown on a passive Ge substrate according to a conventional
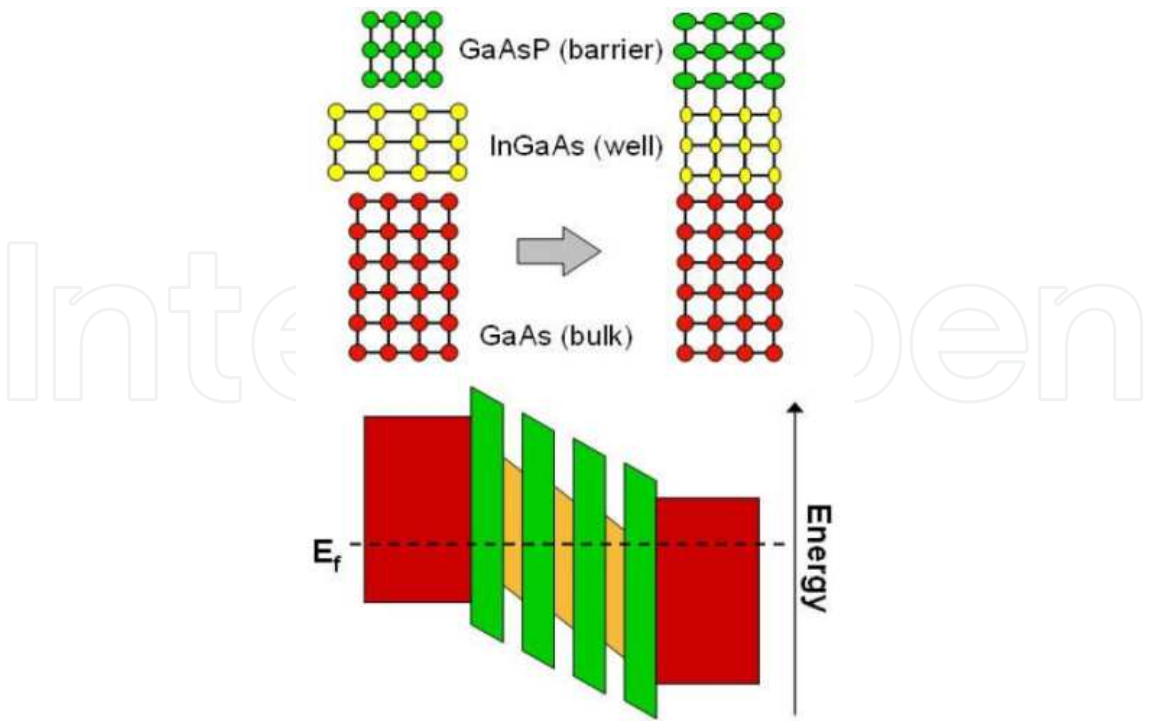
Figure 16. The energy band structure of three strain balanced quantum wells in GaAs solar cells

GaAs cell in order to create a control cell device. The control top cell was grown poorly due to an insufficient thickness of the *p-i-n* top cell. A schematic of the InGaP/GaAs tandem solar cells devices structure is shown in Figure17. [12]
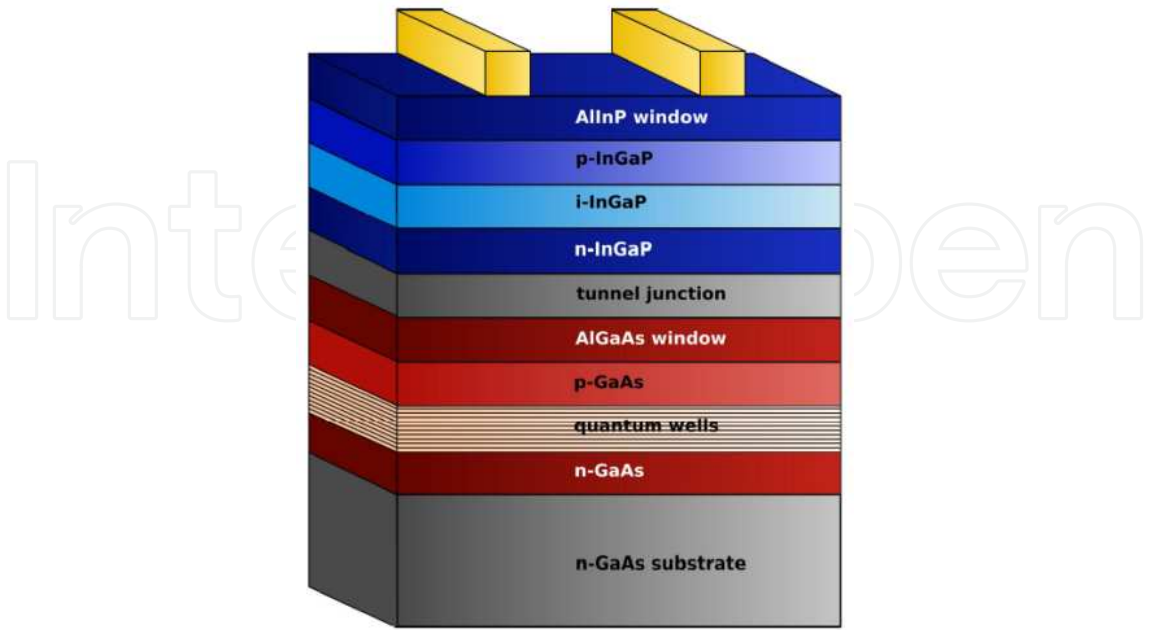

Figure 17. A cross section of the InGaP/GaAs tandem quantum well solar cells devices structure

All solar cells devices were processed for quantum efficiency measurements, fully metalized devices for dark current measurements, and concentrator devices were prepared from each wafer.

4.2. SBQW solar cells simulation results

The external quantum efficiency of the two tandem solar cells devices was characterized as described in [43], their results are shown in Figure 18. Left curves which are from top to bottom in Figure 18 are the top cell of first cell, the control top cell and the top cell of second cell with quantum wells, respectively, right curves which are from top to bottom in Figure 18 are the bottom cell of first cell, the control bottom cell and the bottom cell of second cell with quantum wells, respectively. The lower In content of InGaAs in the second cell with quantum wells improves their band gap. Thus the exciton absorption peaks of the second cell at 922 nm compared to 932 nm for the first cell.
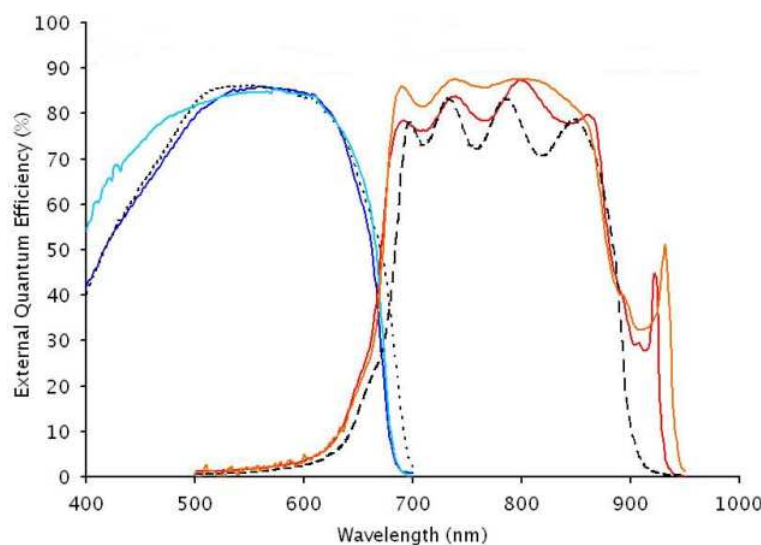

Figure 18. The external quantum efficiency of the tandem control cells and quantum wells cells devices

The Shockley injection currents and Shockley-Read-Hall dark currents of two tandem solar cells devices are simulated using drift diffusion model. The radiative component of the dark currents is calculated from the generalized Planck formula with no free parameters. [44] The conversion efficiency of first cell was independently measured 22.1 ± 0.7 % under low aerosol optical depth, as is shown in Figure 19. The light current curves of top and bottom cell have been constructed by subtracting the dark current of each cell by using the short circuit current measurement at Fraunhofer. These currents weren't mismatch between the top cell and bottom cell calculated by internal quantum conversion efficiency measurement.

Because the top cell emitter doping is lower, the conversion efficiency of first cell is 27.2%. Extrapolating the model for the dark current to higher concentrations, the conversion efficiency of first cell with no series resistance losses would have achieved 29.8% under low aerosol optical depth. The second cell was grown with the higher top cell emitter doping to overcome
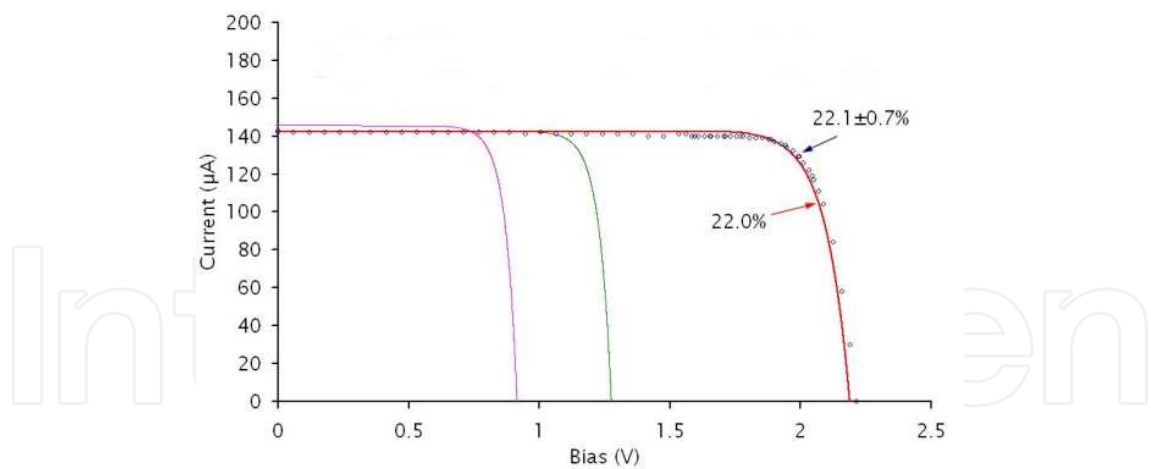
Figure 19. Tandem devices dark current model results relative to the light current curve measured at Fraunhofer

the series resistance of the first cell. The quantum well band gap was increased to counter the production of current in the quantum wells solar cells. Concentrator measurements have been performed on the second solar cells. The results in Table 1 show the conversion efficiencies recorded for both solar cells devices.

The superior photoelectric performance of the quantum wells control solar cells devices in Table 1 could be illustrated by function of the Xenon spectrum wavelengths and the resultant short circuit currents intensity in Figure 20. In the second solar cells devices, the current intensity of limiting bottom cell is improved in the condition of the Xenon spectrum illumination, the current is matched with the control solar cells devices under low aerosol optical depth. The top cell of the second solar cells limited and controlled performs of the quantum wells solar cells devices, because the top cell spectral response can extend to longer wavelengths.

Device	Fill Factor (%)	Efficiency (%)
The second solar cell	81.5	30.4
The control solar cell	81.7	31.6

Table 1. The measured photoelectric performance of the quantum wells control solar cells devices.

Figure 21 shows the quantum wells solar cells could perform over the control solar cells under concentrator spectrum and could perform better over the top solar cells with a larger spectral response. The control solar cells were grown on Ge substrate but the quantum wells solar cells were grown on GaAs substrate. It is known that growth of InGaP would give rise to a higher order degree in the arrangement of In and Ga atoms which could lower the InGaP band gap. [45]The most likely cause is the discrepancy between the top solar cells and optimized design of the InGaP/GaAs quantum wells tandem solar cells.
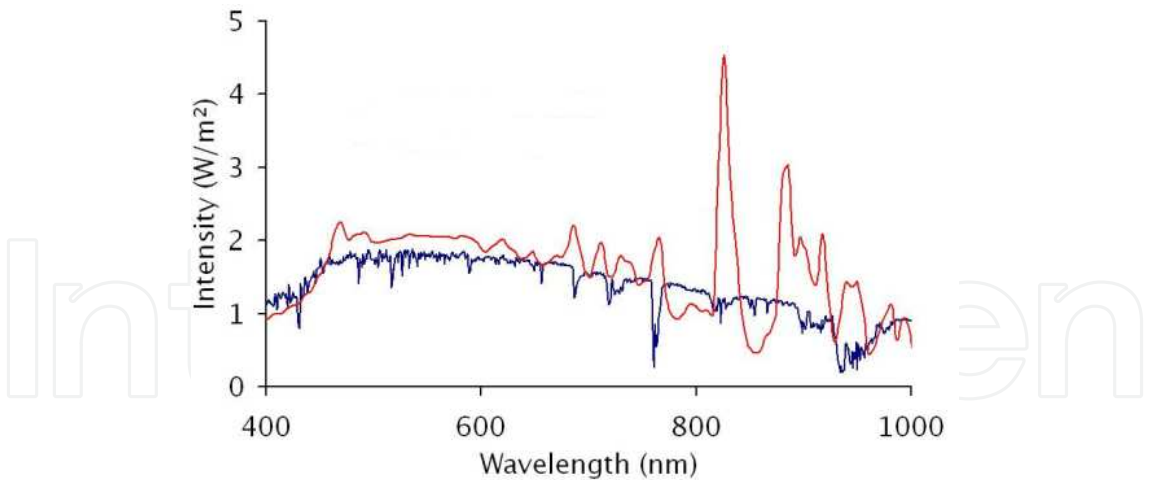
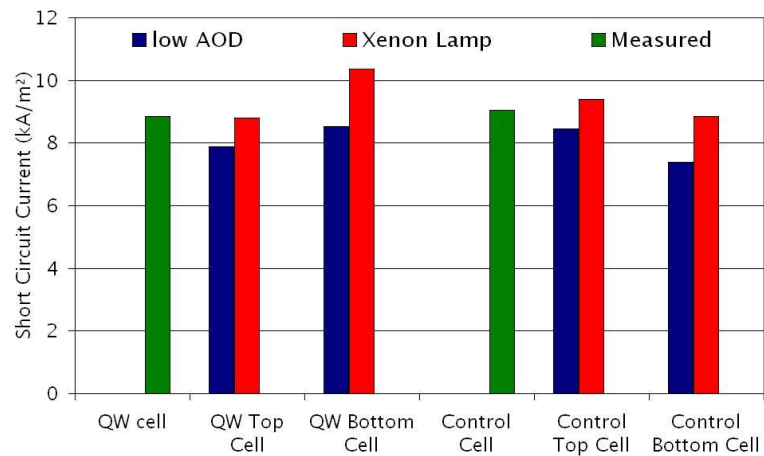**Figure 20.** The Xenon spectrum used to characterize the second solar cells alongside a concentrator spectrum

Figure 21. Short circuit currents under a xenon lamp spectrum and calculated from spectral response curves.
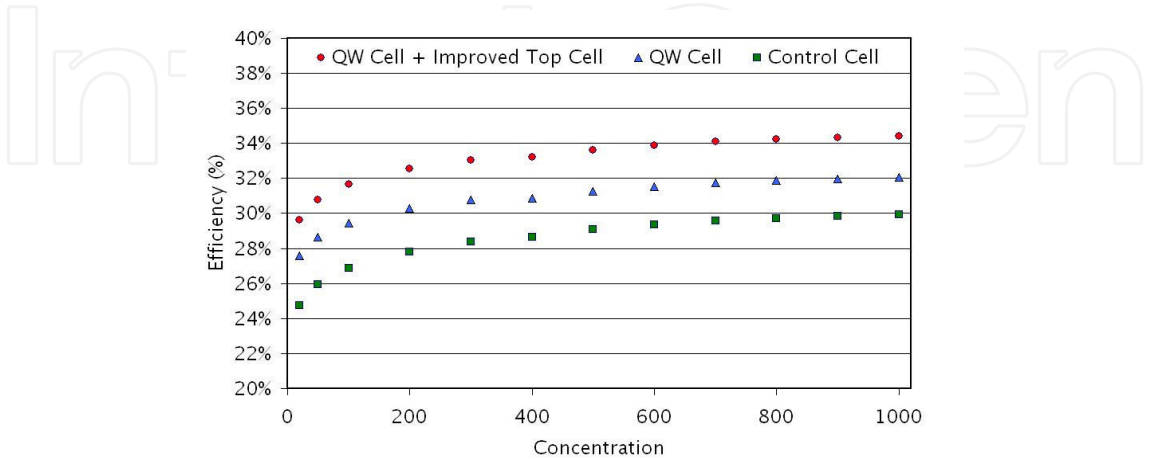

Figure 22. Efficiency predictions under the assumption of additives and a low aerosol optical depth spectrum

To investigate further the performance of the quantum wells solar cells and control solar cells, the conversion efficiency and dark currents have been combined under the assumption of additives and a low aerosol optical depth spectrum, as shown in Figure 22. The red dots show an improved tandem solar cells structure where the top control solar cell with high disorder is grown on the quantum well bottom solar cell. Such solar cells structure should achieve a conversion efficiency of over 34%.

5. Conclusions

In this chapter, the structure characteristics and optoelectronic properties of InGaN/GaN multiple quantum wells solar cells with In content about 0.3 and 0.4 are analyzed and studied, the phase separation of GaN and InN are not observed in the InGaN alloy materials with all kinds of In content when the InGaN alloys materials are packaged by InGaN/GaN multiple quantum wells heterojunction. The open circuit voltage of InGaN/GaN multiple quantum wells solar cells with In content about 0.3 and 0.4 are measured by 2 V and 1.8 V, respectively, when InGaN alloys materials are irradiated by monochromatic light under the same white light source. The InGaN/GaN multiple quantum wells are used as solar cells excitation region, the fill factor of this solar cell is about 0.6. The external quantum efficiency of this solar cell is 40% at the wavelength 420 nm, but external quantum efficiency drops to only 10% at the wavelength of 450 nm.

The performance of InP/InGaAsP quantum wells solar cells can be greatly improved by integration of dielectric or metal nanoparticles into the surface of the tandem solar cells devices structure in order to couple incident light into the lateral propagation paths which can confine the slabby waveguide formed by the multiple quantum wells intrinsic layer. This approach can also improve the inherent conflict in achieving both efficient photon absorption which mandated a thick multiple quantum wells layer and efficient collection of the photo-generate carriers which required a thin multiple quantum wells layer, and could further realize the high optoelectronic conversion efficiency predicted for InP/InGaAsP quantum wells tandem solar cells.

It has been known that quantum wells can tailor bandedges absorption, which also provides the flexibility to currently match InGaP/GaAs tandem solar cells under any defined spectrum. The device conversion efficiency has been achieved to 30.6% under the concentrator spectrum. This is a new record for any nanostructure solar cells devices. Strain balanced quantum wells solar cells with optimized conventional top solar cells should achieve the conversion efficiency of 34%. A new high efficiency consisting of quantum wells tandem solar cells have been proposed in both the GaAs and InGaP solar cells. This solar cells devices structure has the advantage to achieve higher efficiency comparable to the current lattice mismatched multi-junction tandem solar cells.

Acknowledgements

Author details

Shaoguang Dong[1*], Kanghua Chen[1], Guojie Chen[2] and Xin Chen[2]

*Address all correspondence to: dshgfosu@126.com

1 Department of Optoelectronics and Physics, Foshan University, Foshan, China

2 Institute of Science, Foshan University, Foshan, China

References

[1] Neufeld C J, Toledo N G, Cruz S C, Iza M, DenBaars S P and Mishra U K. High quantum efficiency InGaN/GaN solar cells with 2.95 eV band gap. Applied Physics Letters 2008; 93: 143502.

[2] Tsai, Y L, Lin C C, Han H V, Chen H C, Chen K J, Lai W C, Sheu J K, Lai F I and Yu P C. Efficiency enhancement of InGaN/GaN multiple quantum well solar cells using CdS quantum dots and distributed Bragg reflectors, Physics Simulation and Photonic Engineering of Photovoltaic Devices II, 2013.

[3] Liou B W. Design and fabrication of $In_xGa_{1-x}N$/GaN solar cells with a multiple-quantum-well structure on SiCN/Si (111) substrates. Thin Solid Films 2011; 520(3): 1084-1090.

[4] Liou B W. Temperature of $In_xGa_{1-x}N$/GaN solar cells with a multiple-quantum-well structure on SiCN/Si(111) substrates. Solar Energy Materials & Solar Cells 2013; 114: 141–146.

[5] Chang S H, Fang Y K, Ting S F. Poly- and single-crystalline h-GaN grown on SiCN/Si(100) and SiCN/Si(111) substrates by MOCVD. Journal of Electronic Materials 2006; 10: 1837-1841.

[6] Ji L, Lu S L, Wu Y Y, Dai P, Bian L F, Masayuki A, Tomomasa W, Naohiro A, Mitsunori U, Atsushi T, Shiro U and Yang H. Carrier recombination dynamics of MBE grown InGaAsP layers with 1eV bandgap for quadruple-junction solar cells. Solar Energy Materials and Solar Cells 2014; 27: 1-5.

[7]   Kwon Y S. InP/InGaAsP/InP double heterojunction solar cells with increased short-circuit current. Conference Record of the Thirty-first IEEE Photovoltaic Specialists Conference, 2005.

[8]   Derkacs D, Chen W V, Matheu P M, Lim S H, Yu P K L and Yu E T. Nanoparticle-induced light scattering for improved performance of quantum-well solar cells. Applied Physics Letters 2008; 93: 091107.

[9]   Deng Z, Wang R X, Ning J Q, Zheng C C, Bao W, Xu S J, Zhang X D, Lu S L, Dong J R, Zhang B S and Yang H. Radiative recombination of carriers in the $Ga_xIn_{1-x}P/GaAs$ double-junction tandem solar cells. Solar Energy Materials and Solar Cells 2013; 111: 102-106.

[10] Sugaya T, Takeda A, Oshima R, Matsubara K, Niki S and Okano Y. InGaP solar cells fabricated using solid-source molecular beam epitaxy. Journal of Crystal Growth 2013; 378: 576-578.

[11] Tatsuya T, Eiji I, Hiroshi K and Masamichi O. Over 30% efficient InGaP/GaAs tandem solar cells. Applied Physics Letters 1997; 70: 381.

[12] Browne B, Andreas I, James C, Barnham K, John R, Robert A, Hill G, Guy S and Begin J V. Tandem Quantum Well Solar Cells. Photovoltaic Specialists Conference, 2008: 1-5.

[13] Lu T, Kao C, Kuo H, Huang G and Wang S. CW lasing of current injection blue GaN-based vertical cavity surface emitting laser. Applied Physics Letters 2008; 92: 141102.

[14] Dahal R. InGaN/GaN multiple quantum well solar cells with long operating wavelengths. Applied Physics Letters 2009; 94: 063505.

[15] Jani O, Ferguson I, Honsberg C and Kurtz S. Design and characterization of GaN/InGaN solar cells. Applied Physics Letters 2007; 91: 132117.

[16] Vos A D. Endoreversible Thermodynamics of Solar Energy Conversion. Oxford: Oxford University Press; 1992.

[17] Ho I and Stringfellow G B. Solid phase immiscibility in GaInN. Applied Physics Letters 1996; 69(18): 2701-2703.

[18] Pantha B N, Li J, Lin J Y and Jiang H X. Single phase $In_xGa_{1-x}N$ ($0.25 \leq x \leq 0.63$) alloys synthesized by metal organic chemical vapor deposition. Applied Physics Letters 2008; 93: 182107.

[19] Tabata A, Teles L K, Scolfaro L M R, Leite J R, Kharchenko A, Frey T, As D J, Schikora D, Lischka K, Furthmuller J and Bechstedt F. Phase separation suppression in InGaN epitaxial layers due to biaxial strain. Applied Physics Letters 2002; 80(5): 769-771.

[20] Wei G, Shiu K T, Giebink N C and Forrest S R. Thermodynamic limits of quantum photovoltaic cell efficiency. Applied Physics Letters 2007; 91: 223507.

[21] Barnham K W J, Braun B, Nelson J, Paxman M, Button C, Roberts J S and Foxon C T. Short -circuit current and energy efficiency enhancement in a low-dimensional structure photovoltaic device. Applied Physics Letters 1991; 59(1): 135-137.

[22] Raisky O Y, Wang W B, Alfano R R, Reynolds C L, Stampone D V and Focht M W. In$_1$$_xGaxAs_1$$_yPy$/InP multiple quantum well solar cell structures. Journal of Applied Physics 1998; 84(10): 5790-5794.

[23] Alemu A, Coaquira J A H and Freundlich A. Dependence of device performance on carrier escape sequence in multi-quantum-well p-i-n solar cells. Journal of Applied Physics 2006; 99: 084506.

[24] Mohaidat J M, Shum K, Wang W B and Alfano R R. Barrier potential design criteria in multiple- quantum-well-based solar cell structures. Journal of Applied Physics 1994; 76(9): 5533-5537.

[25] Adachi S. Optical dispersion relations for GaP, GaAs, GaSb, InP, InAs, InSb, Al $_x$Ga$_{1-x}$ As, and In$_{1-x}$ Ga $_x$ As $_y$ P$_{1-y}$. Journal of Applied Physics 1989; 66 (12): 6030-6040.

[26] Catchpole K R and Pillai S. Absorption enhancement due to scattering by dipoles into silicon waveguides. Journal of Applied Physics 2006; 100: 044504.

[27] Derkacs D, Lim S H. Matheu P. Mar W and Yu E T. Improved performance of amorphous silicon solar cells via scattering from surface plasmon polaritons in nearby metallic nanoparticles. Applied Physics Letters 2006; 89: 093103.

[28] Lim S H, Mar W, Matheu P, Derkacs D and Yu E T. Photocurrent spectroscopy of optical absorption enhancement in silicon photodiodes via scattering from surface plasmon polaritons in gold nanoparticles. Journal of Applied Physics 2007; 101: 104309.

[29] Sundararajan S P, Grady N K, Mirin N and Halas N J. Nanoparticle-induced enhancement and suppression of photocurrent in a silicon photodiode. Nanoparticle Letters 2008; 8(2): 624-630.

[30] Yeh P. Optical Waves in Layered Media. New York: Wiley-Blackwell; 2005.

[31] Pillai S, Catchpole K R, Trupke T and Green M A. Surface plasmon enhanced silicon solar cells. Journal Applied Physics 2007; 101: 093105.

[32] Schaadt D M, Feng B and Yu E T. Enhanced semiconductor optical absorption via surface plasmon excitation in metal nanoparticles. Applied Physics Letters 2005; 86: 063106.

[33] Soller B J and Hall D G. Energy transfer at optical frequencies to silicon-based waveguiding structures. Journal of the Optical Society America A 2001; 18(10): 2577-2584.

[34] Soller B J, Stuart H R and Hall D G. Energy transfer at optical frequencies to silicon on insulator structures. Optics Letters 2001; 26(18): 1421-1423.

[35] Ward J S, Wanlass M W, Emery K A and Coutts T J. GaInAsP solar cells with the ideal band gap for terrestrial concentrator applications. Proceeding of the 23rd IEEE Photovoltaic Specialists Conference, Louisville; 1993.

[36] Barnham K W J, Abbott P, Ballard I M, Bushnell D B, Connolly J, Ekins-Daukes N, Mazzer M, Nelson J, Rohr C, Tibbits T N D, Airey R, Hill G and Roberts J. Recent Results on Quantum Well Solar Cells. World Conference on Photovoltaic Energy Conversion, Osaka, Japan; 2003.

[37] Bushnell D B, Tibbits T N D, Barnham K W J, Connolly J P, Mazzer M, Ekins- Daukes N J, Roberts J S, Hill G and Airey R. Effect of well number on the performance of quantum-well solar cells. Journal of Applied Physics 2005; 97.

[38] Ptak A J, Friedman D J, Kurtz S R. Enhanced-Depletion-Width GaInNas Solar Cells Grown by Molecular-Beam Epitaxy. Proceeding of the 31st IEEE Photovoltaics Specialists Conference and Exhibition, Lake Buena Vista, Florida; 2005.

[39] King R R. 40% efficient metamorphic GaInP/GaInAs/Ge multijunction solar cells. Applied Physics Letters 2007; 90: 183516.

[40] Tibbits T N D, Ballard I M, Barnham K W J, Ekins-Daukes N J, Airey R, Hill G and Roberts J S. The Potential for Strain Balanced Quantum Well Solar Cells in Terrestrial Concentrator Applications. World Conference on Photovoltaic Energy Conversion, Osaka, Japan; 2003.

[41] Lynch M C, Ballard I M, Bushnell D B, Connolly J P, Johnson D C, Tibbits T N D, Barnham K W J, N. Ekins-Daukes J, Roberts J S, Hill G, Airey R and Mazzer M. Spectral response and III-V characteristics of large well number multi quantum well solar cells. Journal of Materials Science 2005; 40: 1445-1449.

[42] Ekins D N J, Kawaguchi K and Zhang J. Strain-Balanced Criteria for Multiple Quantum Well Structures and Its Signature in X-ray Rocking Curves. Crystal Growth & Design 2002; 2: 287-292.

[43] Ioannides A, Tibbits T N D, Connolly J P, Bushnell D B, Barnham K W J, Calder C, Hill G, Roberts J S and Smekens G. Strain Balanced Multi-Quantum Well Dual Junction Monolithic Tandem Solar Cell. Proceeding of the 21st European Photovoltaic Specialists Conference, Dresden; 2006.

[44] Connolly J P. Efficiency Limits of Quantum Well Solar Cells. Proceeding of the 19th European Photovoltaic Solar Energy Conference, Paris; 2004.

[45] Ernst P. Ordering in GaInP studied by optical spectroscopy. Physica status solidi (c) 1996; 193: 213.